Proc. Indian Acad. Sci. (*Chem. Sci.*), Vol. 114, No. 5, October 2002, pp 461–472

Half-sandwich (η^6-arene)ruthenium(II) chiral Schiff base complexes: Analysis of the diastereomeric mixtures in solution by 2D-NMR spectroscopy

RAKESH K RATH[a], G A NAGANA GOWDA[b] and
AKHIL R CHAKRAVARTY[a]*
[a] Department of Inorganic and Physical Chemistry, and
[b] Sophisticated Instruments Facility, Indian Institute of Science,
Bangalore 560 012, India
e-mail: arc@ipc.iisc.ernet.in

MS received 16 April 2002

Abstract. 2D NMR spectroscopy has been used to determine the metal configuration in solution of three complexes, viz. [(η^6-*p*-cymene)Ru(L*)Cl] (**1**) and [(η^6-*p*-cymene)Ru(L*)(L′)] (ClO_4) (L′ = H_2O, **2**; PPh_3, **3**), where L* is the anion of (*S*)-(1-phenylethyl)salicylaldimine. The complexes exist in two diastereomeric forms in solution. Both the (R_{Ru},S_C)- and (S_{Ru},S_C)-diastereomers display the presence of attractive CH/π interaction involving the phenyl group attached to the chiral carbon and the cymene ring hydrogens. This interaction restricts the rotation of the C*–N single bond and, as a result, two structural types with either the hydrogen atom attached to the chiral carbon (C*) or the methyl group attached to C* in close proximity of the cymene ring protons get stabilized. Using 2D NMR spectroscopy as a tool, the spatial interaction involving these protons are studied in order to obtain the metal configuration(s) of the diastereomeric complexes in solution. This technique has enabled us to determine the metal configuration as (R_{Ru},S_C) for the major isomers of **1–3** in solution.

Keywords. (Arene)ruthenium(II) complex; chiral Schiff-base; 2D NMR spectroscopy; absolute configuration; diastereomeric mixtures.

1. Introduction

Chiral half-sandwich organometallic complexes are of significant current interest for their use as catalysts in enantioselective organic transformation reactions [1–23]. While the catalytic activity in these reactions is generated by the metal, the auxiliary chiral ligand plays an important role in the stereoselectivity of the process. A crucial aspect in this chemistry is the configurational stability of the metal and the chiral ligand(s). The problem of chiral stability at the metal atom in these half-sandwich complexes has recently been investigated and the results show that the solution behaviour of the configurationally labile metal centre differs from that in the solid state [24–26].

In 1991 we have reported the crystal structure of [(η^6-*p*-cymene)Ru(L*)(PPh_3)](ClO_4) (**3**) [*p*-cymene = 1-isopropyl-4-methylbenzene; L* = anion of (*S*)-(1-phenylethyl)salicylaldimine] [27]. The complex crystallizes in a single diastereomeric form with the metal

*For correspondence

absolute configuration of R_{Ru}. We have subsequently reported the crystal structures of [(η^6-*p*-cymene)Ru(L*)Cl] (**1**) and [(η^6-*p*-cymene) Ru(L*)(H_2O)](ClO_4) (**2**) [28,29]. The chloro and aqua adducts crystallize with two diastereomers of (R_{Ru},S_C)- and (S_{Ru},S_C)-configurations in a 1:1 molar ratio. The complexes **1**–**3**, however, in solution phase, show the presence of two diastereomers in different mole ratios [27–29]. It has been observed that the complexes are configurationally labile and the absolute configuration at the metal in the diastereomers in solution cannot be determined unequivocally from the room temperature CD and NMR spectral data [24–26,30–34]. The present work stems from our interest in assigning the metal configuration correctly in **1–3** in the solution phase. The results are expected to be of general utility for assigning the metal configuration in related half-sandwich complexes [35–38]. We have probed the solution structures of the complexes using 2D NMR spectroscopy [24,39]. This technique has enabled us to correctly analyse the diastereomeric mixtures of **1–3** in solution.

2. Experimental

All the reactions were carried out in dry solvents under dinitrogen atmosphere using the conventional Schlenk technique. Solvents were dried and distilled under dinitrogen prior to use. Dichloromethane and *n*-hexane were purified over calcium hydride and sodium/ benzophenone respectively. The precursor complex [(η^6-*p*-cymene)$RuCl_2$]$_2$ was prepared by a literature procedure [40]. Complexes **1**–**3** were prepared by our reported methods with minor modifications [27–29]. The CHN and ^{1}H NMR spectral data of **1**–**3** were in agreement with the reported values. Solution 1D NMR and 2D COSY, NOESY and ROESY NMR spectra at 293 and 223 K were recorded on FT-Bruker AMX 400 MHz spectrometer using $CDCl_3$ as a solvent. The elemental analysis was done on a Perkin Elmer model 2400 CHN analyser.

2.1 *Preparation of [(S_{Ru},S_C), (R_{Ru},S_C)]-[(η^6-p-cymene)RuCl{O-C_6H_4-2-CH=N-(S)-CH(Me)Ph}] (**1**)*

Complex **1** as a diastereomeric mixture was prepared by reacting 200 mg of [(η^6-*p*-cymene)$RuCl_2$]$_2$ (0·33 mmol) with 150 mg of (*S*)-(–)-α-methylbenzylsalicylaldimine (HL*, 0·67 mmol) and 80 mg of Na_2CO_3 (0·75 mmol) in 10 ml CH_2Cl_2 at 25°C under stirring for 3 h. The mixture was filtered through celite and the filtrate was reduced to a volume of ~5 ml, after which 20 ml *n*-hexane was added to it to precipitate the orange-red solid which was washed thoroughly with *n*-hexane and finally dried in vacuum (Yield: ~95%).

2.2 *Preparation of [(S_{Ru},S_C), (R_{Ru},S_C)]-[(η^6-p-cymene)Ru(L*)(L′)] (ClO_4) (L′ = H_2O, **2**; PPh_3, **3**)*

The aqua and triphenylphosphine adducts of **1** were prepared by following a similar procedure as described below. The diastereomeric mixture of **1** (200 mg, 0·4 mmol) was reacted with $AgClO_4$ (83 mg, 0·4 mmol) in 5 ml CH_2Cl_2 at 0°C for 30 min. The precipitated AgCl was removed by filtration. The yellow aqua adduct **2** was isolated from the filtrate by treatment with a trace quantity of water followed by precipitation of the solid in a quantitative yield on addition of *n*-hexane (10 ml). Complex **3** was obtained by reacting 260 mg (1·0 mmol) of PPh_3 with the filtrate at 0°C and stirring the mixture for

15 min. The solution was concentrated to ~2 ml. Addition of 10 ml *n*-hexane gave the yellow solid adduct of **3** in quantitative yield. The complex was washed thoroughly with n-hexane and dried in vacuum.

Caution! Perchlorate salts of the metal complexes are potentially explosive and should be handled in small quantities with great care.

3. Results and discussion

3.1 *Crystal structures and metal configuration(s)*

The solid state structures of the chloro (**1**), aqua (**2**) and triphenylphosphine (**3**) adducts have earlier been reported by us [27–29]. Perspective views of the molecules are shown in figure 1. Both the chloro and aqua complexes crystallize with two diastereomers having

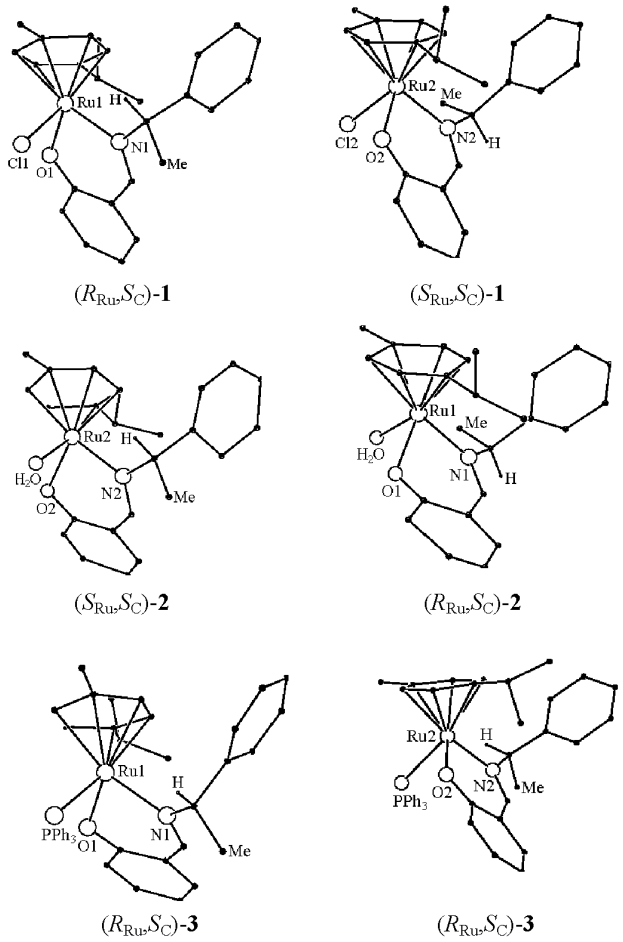

(R_{Ru},S_C)-**1** (S_{Ru},S_C)-**1**

(S_{Ru},S_C)-**2** (R_{Ru},S_C)-**2**

(R_{Ru},S_C)-**3** (R_{Ru},S_C)-**3**

Figure 1. Perspective views of the coordination geometry as observed in the crystal structures of **1–3** showing the presence of (R_{Ru},S_C)- and (S_{Ru},S_C)-configurations for **1** and **2**, and (R_{Ru},S_C)-configuration for **3**.

(S_{Ru},S_C)- and (R_{Ru},S_C)-configurations in a 1:1 molar ratio. The corresponding PPh_3 adduct (**3**) crystallizes with one diastereomer showing (R_{Ru},S_C)-configuration. There are few general observations in the crystal structures of the complexes. First, the phenyl ring attached to the chiral carbon atom of the N,O-donor bidentate chelating salicylaldimine ligand is directed towards the cymene ring in both the diastereomers of **1** and **2** showing (S_{Ru},S_C)- and (R_{Ru},S_C)-configurations and in the (R_{Ru},S_C)-isomer of **3**. The C(sp^2)H/π interaction between the η^6-arene and a phenyl group has a stabilizing effect on the structure. The profound influence of this effect involving a β-phenyl group and a η^5-cyclopentadienyl or η^6-arene ring in analogous half-sandwich transition metal complexes has earlier been reported [33,39,41–48]. Secondly, the hydrogen atom attached to the chiral carbon atom which lies nearly on the ligand plane is directed towards the cymene ring in the (R_{Ru},S_C)-isomer of **1** and (S_{Ru},S_C)-isomer of **2**. The same hydrogen is directed away from the cymene ring in the (S_{Ru},S_C)-isomer of **1** and (R_{Ru},S_C)-isomer of **2**. The metal configuration is based on the priority sequence of the ligands [49]. The third observation is that the methyl group attached to the chiral carbon is directed towards the cymene ring in (S_{Ru},S_C)-**1** and (R_{Ru},S_C)-**2**, while this group is projected away from the cymene ring in (R_{Ru},S_C)-**1** and (S_{Ru},S_C)-**2**.

The CH/π interaction in complexes **1**–**3** is likely to restrict the rotation around the C*–N bond (C*, chiral carbon) [39]. Based on the structural results and considering the presence of CH/π attractive interaction, the diastereomers are classified into two general structural types, viz. (I) and (II) as shown in figure 2. Determination of the structural types of the diastereomeric species in solution can be made on the basis of the interaction of the protons C*–H or C*–Me with the protons of the cymene ring. Selected spatial separations suitable for 2D-NMR studies are listed in table 1. We have attempted to probe such interactions in the solution phase by 2D NMR spectroscopy [33,39,50,51].

3.2 *2D NMR spectral studies*

The ^{1}H NMR spectra of **1**–**3** are shown in figure 3. The spectral feature show the appearance of the *p*-cymene ring protons as doublets in the range δ 4·0–6·0 ppm. The methyl and isopropyl methyl protons of this ligand appear as singlet and doublets in the δ range 1·0–3·0 ppm. The septet corresponding to the isopropyl proton is observed near

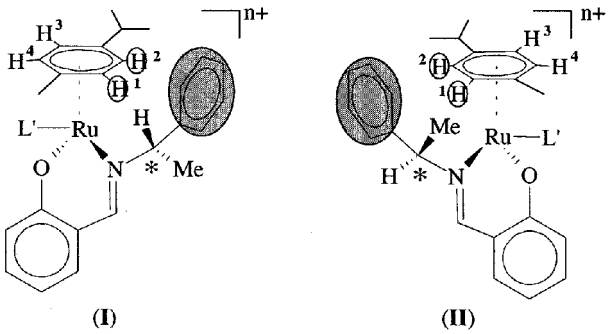

Figure 2. Structural types (I) and (II) showing non-covalent CH/π attractive interaction (L′ = Cl, n = 0; L′ = H_2O or PPh_3, n = 1).

Table 1. ^{1}H NMR data[a] in $CDCl_3$ at 293 K for the major and minor diastereomers of [(η^6-*p*-cymene)Ru(L*)Cl] (**1**) and [(η^6-*p*-cymene)Ru(L*)(L′)](ClO_4) (L′ = H_2O, **2**; PPh_3, **3**) [δ, ppm (multiplicity, $^3J_{HH}$ in Hz, number of protons)].

Complex	*p*-Cymene	L*	L′
1	*Major isomer:* 1·10, 1·14 (*d*, 8, 6H), 2·10 (*s*, 3H), 2·67 (*sp*, 8, 1H), 4·75, 4·95, 5·13, 5·25 (*d*, 7, 4H) *Minor isomer:* 1·12, 1·25 (*d*, 8, 6H), 2·16 (*s*, 3H), 2·82 (*sp*, 8, 1H), 5·12, 5·30, 5·40, 5·51 (*d*, 7, 4H)	*Major isomer:* 1·76 (*d*, 8, 3H), 5·90 (*q*, 7, 1H), 6·46 (*t*, 7, 1H), 6·99 (*m*, 2H), 7·18 (*t*, 7, 1H), 7·45 (*m*, 5H), 7·96 (*s*, 1H) *Minor isomer:* 1·98 (*d*, 8, 3H), 5·66 (*q*, 7, 1H), 6·33 (*t*, 7, 1H), 6·75–7·7 (*m*, 8H), 7·6 (*s*, 1H)	
2[b]	0·79, 0·92 (*d*, 8, 6H), 2·18 (*s*, 3H), 2·37 (*sp*, 8, 1H), 4·78, 5·01, 5·48, 5·59 (*d*, 6, 4H)	1·84 (*d*, 8, 3H), 6·01 (*q*, 7, 1H), 6·43 (*t*, 7, 1H), 6·61, 6·76 (*d*, 7, 2H), 7·05 (*t*, 7, 1H), 7·42 –7·51 (*m*, 5H), 7·68 (*s*, 1H)	3·90 (*br*)
3	*Major isomer:* 0·82, 1·06 (*d*, 8, 6H), 1·59 (*s*, 3H), 2·37 (*sp*, 7, 1H), 4·63 (*d*, 7, 1H), 5·20, 5·34 (*d*, 6, 2H), 5·45 (*d*, 7, 1H) *Minor isomer:* 0·98, 1·13 (*d*, 8, 6H), 2·09 (*s*, 3H), 2·65 (*sp*, 7, 1H), 4·74, 4·94, 5·13, 5·24 (*d*, 7, 4H)	*Major isomer:* 1·29 (*d*, 8, 3H), 5·53 (*q*, 8, 1H), 6·33 (*t*, 7, 1H), 6·74 (*m*, 2H), 7·07 (*t*, 7, 1H), 7·28–7·60 (*m*, 5H), 7·78 (*s*, 1H) *Minor isomer:* 1·72 (*d*, 8, 3H), 5·89 (*q*, 8, 1H), 6·44 (*t*, 7, 1H), 6·96–7·64 (*m*, 8H), 7·95 (*s*, 1H)	*Major isomer:* 7·40–7·60 (*m*, 15H) *Minor isomer:* 7·27–7·56 (*m*, 15 H)

[a] Multiplicity: *br*, broad; *d*, doublet; *q*, quartet; *m*, multiplet; *s*, singlet; *sp*, septet; *t*, triplet. HL*, (*S*)-(1-phenylethyl)salicylaldimine. [b] The complex is present as an essentially pure diastereomer in solution

δ 2·5 ppm. The imine and phenyl ring protons of the Schiff base show peaks in the aromatic region. The C*–H and C*–Me, where C* is the chiral carbon of the Schiff base, display signals around δ 6·2 and 1·8 ppm, respectively.

The spectrum of complex **1** in $CDCl_3$ at –50°C shows the presence of two diastereomers in a ratio of 85:15. The NOESY spectrum of **1** for the δ range 4·5 to 6·0 ppm is displayed in figure 4. In the major diastereomer, the proton attached to the chiral carbon viz. C*–H which appears at δ 5·90 ppm exhibits NOE cross peaks with the cymene ring protons (δ 4·75–5·25 ppm). The major isomer does not show any NOE cross peaks between the methyl protons of C*-Me (δ 1·75 ppm) and the cymene ring protons. This indicates the structural type-(I) for the major diastereomer of **1** with a (R_{Ru},S_C)-configuration based on the priority order: cymene > Cl > O (L*) > N (L*) (figure 2). The minor isomer of **1** does not show any NOE cross peaks between C*–H (δ 5·66 ppm) and the cymene ring protons. However, the methyl protons of C*–Me (δ 1·95 ppm) in the minor isomer display significant NOE cross peaks with the cymene protons (δ 5·12–5·51 ppm) (figure 4). The 2D NMR data suggest a structural type-(II) for the minor isomer with a (S_{Ru},S_C)-configuration (figure 2). The presence of NOE cross peaks which

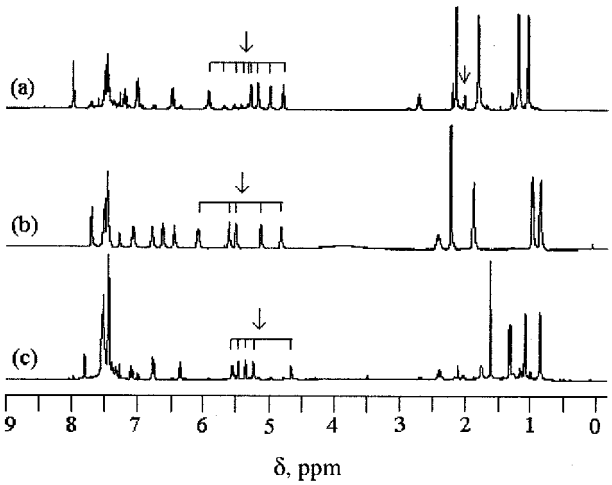

Figure 3. 400 MHz ^{1}H NMR spectra of **1–3** in $CDCl_3$ at 293 K displaying the diastereomeric ratios of 85:15 for **1** (**a**), an essentially pure **2** (**b**) and 98:2 for **3** (**c**). Diagnostic signals used for 2D NMR measurements are indicated by arrow in the spectra.

Table 2. Selected spatial separations (Å) in the complexes **1–3**.

	(R_{Ru},S_C)-**1**	(S_{Ru},S_C)-**1**	(R_{Ru},S_C)-**2**	(S_{Ru},S_C)-**2**	(R_{Ru},S_C)-**3**
Cymene/Ph(C) interaction*[a]					
C^0_{Ph}...H^1	3·528	3·399	3·739	3·875	2·669
C^0_{Ph}...H^2	3·100	2·978	3·113	2·788	3·618
C^0_{Ph}...H^3	6·913	6·944	6·811	6·862	6·978
C^0_{Ph}...H^4	7·160	7·112	7·353	7·143	6·536
Cymene/H(C) interaction*					
C*H...H^1	2·452	4·286	4·545	2·982	3·314
C*H...H^2	3·512	4·327	4·647	3·329	4·535
C*H...H^3	5·616	6·813	6·753	5·786	6·175
C*H...H^4	5·040	6·704	6·895	5·339	5·349
Cymene/Me(C) interaction*[b]					
C*Me...H^1	4·563	3·329	3·300	4·952	4·830
C*Me...H^2	5·074	4·380	4·426	4·678	5·358
C*Me...H^3	7·210	6·437	6·370	7·103	7·343
C*Me...H^4	6·857	5·662	5·843	6·987	6·974
*Distance from the monodentate ligand, L′ (L′ = Cl, **1**; H_2O, **2**; PPh_3, **3**)*					
L′...H(C*)	3·301	4·369	4·089	3.039	3·523
L′...Me(C*)	4·222	3·449	3·069	4.114	4·651
L′...Me_{Cym}[b]	3·511	3·555	3·365	3.268	4·067
L′...C(^{i}Pr)[c]	5·670	5·613	5·539	5.540	5·591

[a] C^0_{Ph}, Centroid of the arene ring attached to C* (the numbering scheme of the cymene ring protons are shown in figure 2)
[b] Me_{Cym}, methyl group of the *p*-cymene ligand
[c] C(^{i}Pr) is the secondary carbon of the isopropyl group of the *p*-cymene ligand

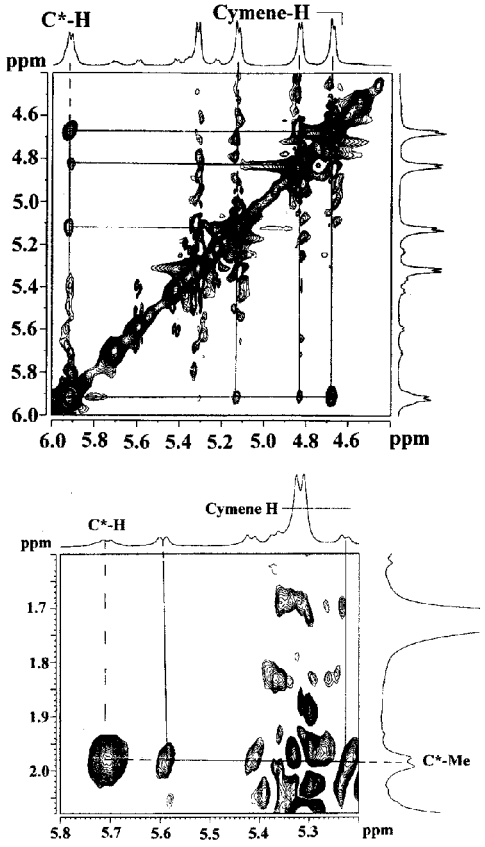

Figure 4. 400 MHz ^{1}H NOESY spectrum of [(η^6-*p*-cymene)Ru(L*)Cl] (**1**) in $CDCl_3$ at –50°C for the major (top) and minor (bottom) diastereomers.

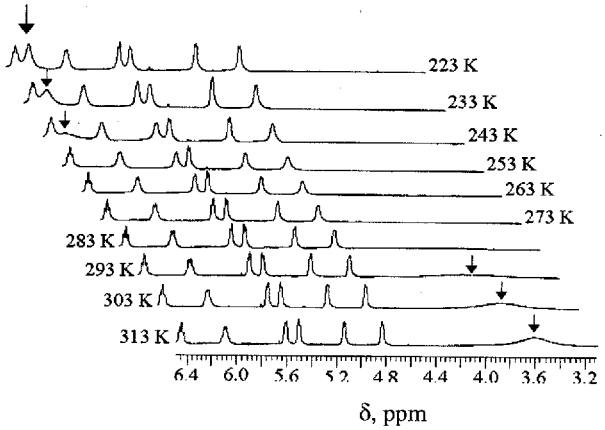

Figure 5. Variable temperature (223–313 K) 400 MHz ^{1}H NMR spectra of the aqua adduct **2** in $CDCl_3$. The arrow indicates the signal for the aqua ligand.

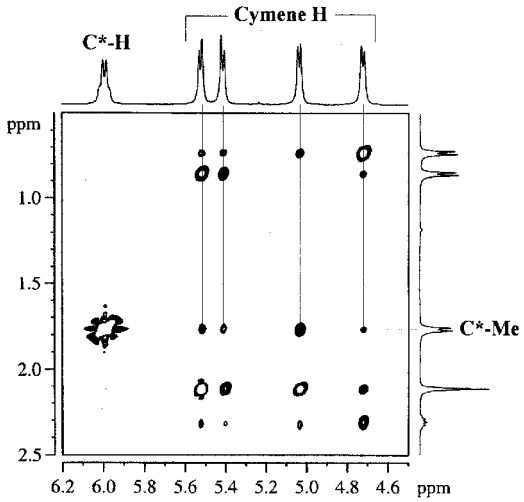

Figure 6. 400 MHz ^{1}H ROESY spectrum of [(η^6-*p*-cymene)Ru(L*)(H_2O)](ClO_4) (**2**) in $CDCl_3$ at 20°C.

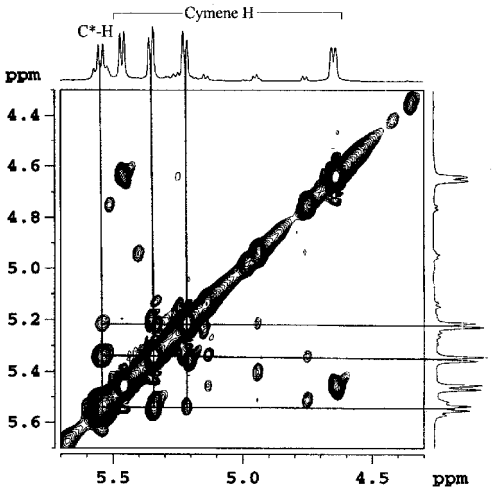

Figure 7. 400 MHz ^{1}H NOESY spectrum of [(η^6-*p*-cymene)Ru(L*)(PPh_3)](ClO_4) (**3**) in $CDCl_3$ at 20°C for the major diastereomer.

arise due to dipolar interaction are indicative of the spatial proximity of the protons[20]. The present work corrects the previously assigned (S_{Ru})-configuration for the major isomer of **1**[28].

The aqua adduct **2** exists in an essentially pure diastereomeric form in solution. The protons of the aqua ligand appear as a broad peak at δ 3·9 ppm in the spectrum recorded at room temperature. At –50°C, the aqua ligand display a relatively sharp peak at δ 6·3 ppm. It is observed that with a decrease in temperature, the peak corresponding to the

aqua ligand at δ 3·9 ppm at 25°C starts broadening with a downfield shift. An upfield shift of the peak is again observed on increasing the temperature. The signal intensity diminishes significantly at 0, –10 and –20°C and reappears as a broad peak centering at δ 6·3 ppm at –30°C (figure 5). The peak tends to become sharp at δ 6·3 ppm on reducing the temperature to –50°C. This could be due to the presence of an equilibrium involving two species having the water molecule in a bound and non-bound state in the complex **2**.

The ^{1}H ROESY spectrum of the aqua adduct in $CDCl_3$ at 20°C shows NOE cross peaks between C*–Me (δ 1·84 ppm) and four cymene ring protons (δ, 4·79–5·90 ppm) (figure 6). The C*–H proton (δ 6·10 ppm) exhibits only a weak NOE cross peak with a cymene ring proton. The major diastereomer of **2** in solution belongs to the structural type-(II) giving a (R_{Ru},S_C)-configuration based on the priority order: cymene > O (L^{15}) > O (H_2O) > N (L^{15}) [29].

The ^{1}H NMR spectrum of **3** shows the presence of two diastereomers in solution in a 98:2 ratio. The ^{1}H NOESY spectrum of **3** exhibits NOE cross peaks between C*–H and the cymene ring protons in the major isomer (figure 7). This indicates a close proximity of C*–H proton to the cymene ring and a structural type-(I) with a (R_{Ru},S_C)-configuration for the major isomer with a priority order: cymene > P (PPh_3) > O (L*) > N (L*) (figure 2). The same configuration is observed for **3** in the crystal structure.[27]

The 2D NMR results show a (R_{Ru})-configuration for all the major diastereomer of **1–3** in solution. Determination of metal configuration is based on the priority order of the ligands. Complexes **1–3** are stereochemically different. While the chloro and the PPh_3

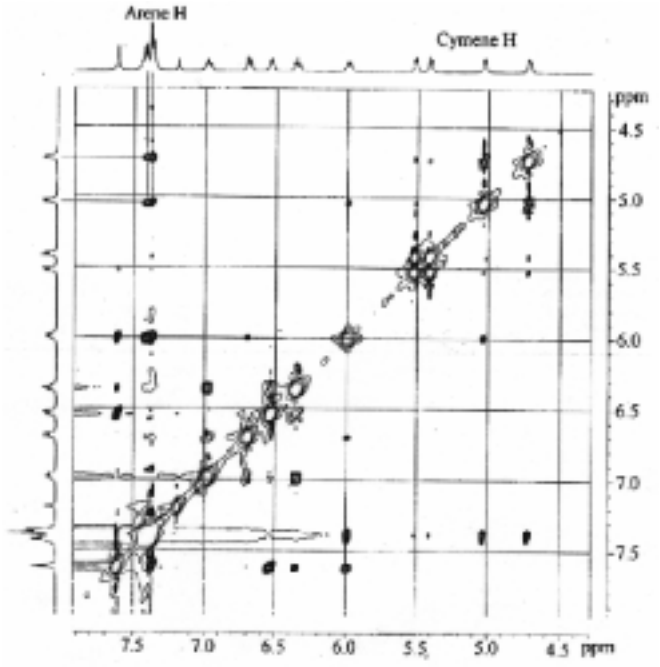

Figure 8. 400 MHz ^{1}H ROESY spectrum of the aqua complex (**2**) displaying the NOE cross peaks between the cymene ring protons and the protons of the phenyl group attached to C*.

ligands in **1** and **3** show a 'proximity' of the monodentate ligand to the hydrogen attached to the chiral carbon (C*), the aqua ligand in **2** is 'proximal' to the methyl group attached to C* atom. This may be related to the steric effect generated by the bulk of the monodentate ligand on the ancillary chelating chiral Schiff base. The dual factors that play important roles are (i) the stabilizing β-phenyl effect in which NOE cross peaks are observed involving two cymene ring protons and the phenyl group attached to the chiral carbon (figure 8) [52,53] and (ii) the destabilizing steric effect involving the adduct ligand. Based on the 2D NMR spectral data it can be inferred that the conversions (R_{Ru},S_C)-**1** → (R_{Ru},S_C)-**2** and (R_{Ru},S_C)-**2** → (R_{Ru},S_C)-**3** associate in the stabilization of the other structural arrangement. This means that (R_{Ru})-**1**, having the hydrogen attached to the chiral carbon (C*) in proximity to Cl, on removal of the halide by H_2O stabilizes (R_{Ru})-**2** with the methyl bonded to C* in proximity to H_2O. Similarly, substitution of H_2O in (R_{Ru})-**2** by PPh_3 (**3**) stabilizes (R_{Ru})-**3** with H (C*) in proximity to PPh_3. A point to note here is that the conversions of (R_{Ru},S_C)-**1** to (R_{Ru},S_C)-**2** and (R_{Ru},S_C)-**2** to (R_{Ru},S_C)-**3** involve a change of relative metal configuration due to a change in priority sequence: cymene > Cl or P > O (L*) > O (H_2O) > N (L*) [49]. The more stable species in the equilibrium, viz. (R_{Ru},S_C)-complex (**1**–**3**) □ (S_{Ru},S_C)-complex (**1**–**3**), is the major diastereomer observed in the solution phase [24–26,31–34,39].

4. Conclusion

The half-sandwich (η^6-*p*-cymene)ruthenium(II) complexes containing a chiral N,O-donor chelating Schiff base (*S*)-(1-phenylethyl)salicylaldimine show the presence of two diastereomers in solution differing only in the metal configuration giving mole ratios of 85:15 for **1**, 98:2 for **3** and an essentially pure aqua adduct **2**. The solid state structures, however, exhibit the presence of two diastereomers in a 1:1 ratio for the chloro and aqua adducts, and a single diastereomer for the PPh_3 adduct. Both the diastereomers having (R_{Ru},S_C)- and (S_{Ru},S_C)-configurations are stabilized by CH/π attractive interaction involving the phenyl group attached to the chiral carbon and the cymene ring.

The 2D NMR spectra of the complexes **1–3** show the spatial interactions of the cymene ring protons with either the H or Me proton(s) attached to the chiral carbon. The major isomer in the chloro adduct displays a 'proximal' arrangement of C*–H with the cymene ring suggesting (R_{Ru},S_C)-configuration for the major diastereomer in solution. The aqua adduct **2**, however, shows NOE cross peaks between C*–Me and cymene ring protons indicating (R_{Ru},S_C)-configuration in the major diastereomer. The NOE cross peaks between C*–H and the cymene ring protons in the PPh_3 adduct **3** indicate a (R_{Ru},S_C)-configuration for the major diastereomer. With the help of the single crystal X-ray structural data, the 2D NMR spectroscopic technique has enabled us to determine the configuration of the major and minor diastereomers of **1–3** in a solution phase.

Acknowledgement

We thank the Council of Scientific and Industrial Research (CSIR) New Delhi, for financial support. Thanks are due to Prof. K L Sebastian and Ms Bidisa Das for helpful discussions.

References

1. Noyori R 1994 *Asymmetric catalysis in organic synthesis* (New York: Wiley-Interscience)
2. Ohkuma T and Noyori R 1999 In *Comprehensive asymmetric catalysis* (eds) E N Jacobsen, A Pfaltz and H Yamamotto (New York: Springer) vol. 1 p. 199
3. Kitamura M, Yoshimura M, Kanda N and Noyori R 1999 *Tetrahedron* **55** 8769
4. Mikami K, Korenaga T, Tereda M, Ohkuma T, Pham T and Noyori R 1999 *Angew. Chem., Int. Ed.* **38** 495
5. Noyori R and Hashiguchi S 1997 *Acc. Chem. Res.* **30** 97
6. Petra D G I, Reek J N H, Handgraff J W, Meijer E J, Dierkes P, Kamer P C J, Brussee J, Schoemaker H E and van Leeuwen P W N M 2000 *Chem. Eur. J.* **6** 2818
7. Petra D G I, Kamer P C J, van Leeuwen P W N M, Goulbitz K, Loon A M V, Vries J G D and Schoemaker H E 1999 *Eur. J. Inorg. Chem.* 2335
8. Braunstein P, Naud F and Rettig S J 2001 *New J. Chem.* **25** 32
9. Braunstein P, Fryzuk M D, Naud F and Rettig S J 1999 *J. Chem. Soc., Dalton Trans.* 589
10. Brunner H 1980 *Adv. Organomet. Chem.* **18** 151
11. Brunner H and Prommesberger M 1998 *Tetrahedron: Asymmetry* **9** 3231
12. Brunner H 1979 *Acc. Chem. Res.* **12** 251
13. Laxmi Y R S and Backvall J E 2000 *Chem. Commun.* 611
14. Katho A, Carmona D, Viguri F, Remacha C D, Kovacs J, Joo F and Oro L A 2000 *J. Organomet. Chem.* **593–594** 299
15. Bernard M, Delbecq F, Sautet P, Fache F and Lemaire M 2000 *Organometallics* **19** 5715
16. Everaere K, Carpentier J F, Mortreux A and Bulliard M 1999 *Tetrahedron: Asymmetry* **10** 4663
17. Davies D L, Fawcett J, Garratt S A and Russell D R 2001 *Organometallics* **20** 3029
18. Davenport A J, Davies D L, Fawcett J, Garratt S A and Russell D R 2000 *J. Chem. Soc., Dalton Trans.* 4432
19. Faller J W and Parr J 2000 *Organometallics* **19** 1829
20. Ritleng V, Sutter J P, Pfeffer M and Sirlin C 2000 *Chem. Commun.* 129
21. Harlow K J, Hill A F and Wilton-Ely J D E T 1999 *J. Chem. Soc., Dalton Trans.* 285
22. Faller J W and Lavoie A 2001 *J. Organomet. Chem.* **630** 17
23. Faller J W, Grimmond B J and D'Alliessi D J 2001 *J. Am. Chem. Soc.* **123** 2525
24. Brunner H 2001 *Eur. J. Inorg. Chem.* 905
25. Brunner H 1999 *Angew. Chem., Int. Ed.* **38** 1194
26. Brunner H and Zwack T 2000 *Organometallics* **19** 2423
27. Mandal S K and Chakravarty A R 1991 *J. Organomet. Chem.* **417** C59
28. Mandal S K and Chakravarty A R 1992 *J. Chem. Soc., Dalton Trans.* 1627
29. Mandal S K and Chakravarty A R 1993 *Inorg. Chem.* **32** 3851
30. Brunner H, Oeschey R and Nuber B 1995 *Inorg. Chem.* **34** 3349
31. Brunner H, Neuhierl T and Nuber B 1998 *Eur. J. Inorg. Chem.* 1877
32. Brunner H, Valério C and Zabel M 2000 *New J. Chem.* **24** 275
33. Brunner H, Oeschey R and Nuber B 1996 *J. Chem. Soc., Dalton Trans.* 1499
34. Brunner H, Köllnberger A, Burgemeister T and Zabel M 2000 *Polyhedron* **19** 1519
35. Attar S, Nelson J H, Fischer J, deClan A, Sutter J-P and Pfeffer M 1995 *Organometallics* **14** 4559
36. Attar S, Catalano V J and Nelson J H 1996 *Organometallics* **15** 2932
37. Maneghetti M R, Grellier M, Pfeffer M, Dupont J and Fischer J 1999 *Organometallics* **18** 5560
38. Loza M L, Parr J and Slawin A M Z 1997 *Polyhedron* **16** 2321
39. Brunner H 1983 *Angew. Chem., Int. Ed. Engl.* **22** 897
40. Bennet M A, Huang T N, Matheson T W and Smith A K 1985 *Inorg. Synth.* **21** 75
41. Brunner H and Lukas R 1979 *Chem. Ber.* **112** 2528
42. Brunner H, Bauer I and Lukas R 1979 *Z. Naturforsch* **B34** 1419
43. Brunner H and Rastogi D K 1980 *Inorg. Chem.* **19** 891
44. Sheldrick W S and Heeb S 1990 *Inorg. Chim. Acta* **168** 93
45. Krämer R, Polborn K, Wanjek H, Zahn I and Beek W 1990 *Chem. Ber.* **123** 767
46. Brunner H, Oeschey R and Nuber B 1996 *Organometallics* **15** 3616

47. Brunner H, Oeschey R and Nuber B 1996 *J. Organomet. Chem.* **518** 47
48. Brunner H, Neuhierl T and Nuber B 1998 *J. Organomet. Chem.* **563** 173
49. Stanley K and Baird M C 1975 *J. Am. Chem. Soc.* **97** 6598
50. Faller J W and Grimmond B J 2001 *Organometallics* **20** 2454
51. Ritleng V, Bertani P, Pfeffer M, Sirlin C and Hirschinger J 2001 *Inorg. Chem.* **40** 5117
52. Yamakawa M, Yamada I and Noyori R 2001 *Angew. Chem., Int. Ed.* **40** 2818
53. Noyori R, Yamakawa M and Hashiguchi S 2001 *J. Org. Chem.* **66** 7931